Bull. Inst. Chem. Res., Kyoto Univ., Vol. 59, No. 2, 1981

Angular Distribution of Slow Positrons from MgO Moderator

Tatsumi MIZOGAWA, Yasuyuki NAKAYAMA, and Tatsumi KAWARATANI*

Received February 14, 1981

The first measurement of the angular distribution of the slow positron beam emitted from a MgO moderator and accelerated to several eV has been performed by connecting the TOF measurements and the measurements of the axial-magnetic-field dependence of slow positron yields. It has been found that the contributions of the non-axial components of the positron velocities to the kinetic energies, which cannot be included in the measured energies by conventional TOF methods, are representatively ~1 eV and not negligibly small in the experiments on the slow positron collisions.

KEY WORDS: Angular distribution/ Low-energy positron/ Moderator/ MgO/ TOF technique/

INTRODUCTION

The study of slow positron collisions with various gases has been in progress since about a decade ago, where the time of flight (TOF) techniques have been playing an important role.[1)]

In general the TOF methods measure the velocity along the axis of the flight path and determine the kinetic energy for each particle, and here the velocity component normal to the axis must be small enough. In the slow positron cases reported so far, however, the magnitude of such component has never been directly measured.

If there exist the intrinsic spreads of kinetic energies and directions of the slow positrons straight away after emitted from the moderator surface, then the slow positron beam after their acceleration to the desired energies will also spread, and hence the normal components will appear. Since the microscopic process of the slow positron emission has not been clearly understood yet, there is no reason to neglect *a priori* the normal component.

In the present work, we have measured the angular distribution of slow positrons emitted from a MgO moderator and accelerated to several eV, using the fact that positrons draw helical paths of which radii are proportional to the normal components of the velocities in axial magnetic field.

EXPERIMENTAL

The schematic diagram of the apparatus is shown in Fig. 1. Basic performance of

* 溝川辰巳, 中山康之, 瓦谷立身: Laboratory of Nuclear Radiation, Institute for Chemical Research, Kyoto University, Kyoto, Japan.

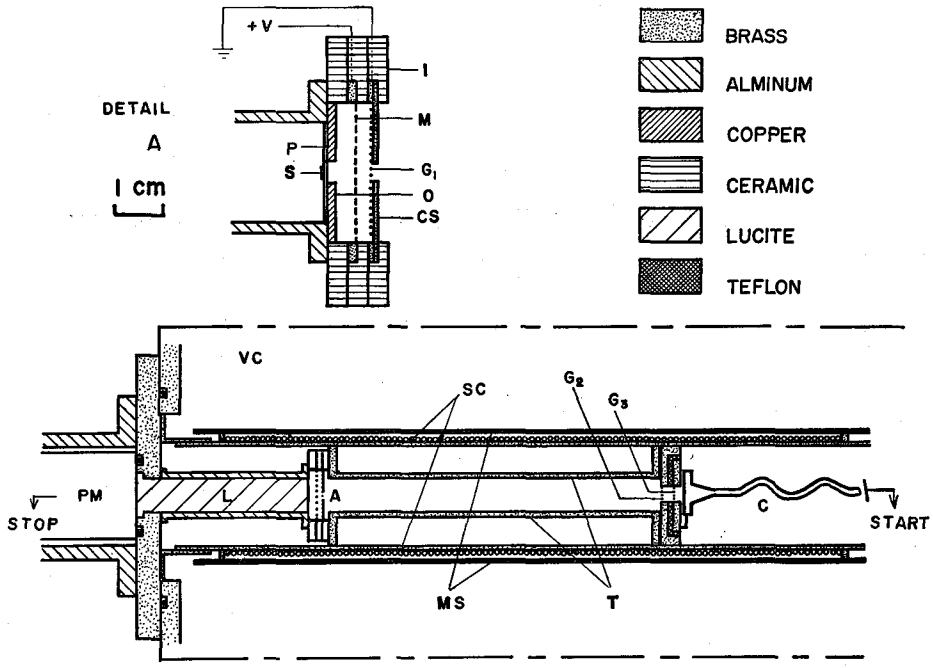

Fig. 1. Schematic diagram of experimental apparatus.
Detail A: to scale. The others: not to scale. A) source assembly, L) Lucite light guide, PM) RCA 8575 photomultiplier, C) Ceratron, VC) vacuum chamber, SC) solenoid coil, MS) μ-metal shield, T) flight tube, G_1, G_2) grounded grids, G_3) grid for positron acceleration to detectable energy (actually -200 V applied), S) ^{22}Na source, and P) plastic scintillator. Right-hand face is deposited with Al for light reflection. The Al-layer is grounded. O) copper disk with 4-mm-diam hole to support the scintillator, M) moderator, CS) brass disk with a 3.2-mm-diam circular slit, and I) ceramic insulators.

the apparatus to measure the flight times of positrons has been described in detail in Ref. 2. For the present work, a 1 mm thick brass disk with a 3.2 mm diam circular slit at the center is set on the righthand side of the grounded grid G_1 to confine the starting places of slow positrons, and a brass tube of 20 mm inner diameter and 20 cm length, which absorbs such positrons that collide with its inner surface, is positioned between the grounded grids G_1 and G_2. The positron detection system, which consists of the grounded grid G_2, negatively biased grid G_3 and a positron detector (Ceratron), and has an effective opening of 1 cm diameter, is mounted at the tube end. The centers of the slit and of the effective opening of the detection system are carefully aligned with the axis of the tube. As a moderator, 200 cell per inch stainless steel grid coated thinly with MgO powder has been used. The MgO powder has been coated by burning magnesium ribbons in air and exposing the stainless steel grid to the smoke. Throughout the experiment the accelerating voltage of 6 V is applied. The stray and earth's magnetic fields are reduced to less than 10 mG in all the flight region by using a 2 mm thick μ metal tube.

PRINCIPLE OF MEASUREMENTS

First we separate a positron kinetic energy E into two terms,

$$E=E_1+E_2, \tag{1}$$

where

$$E_1=\frac{m}{2}v_1^2, \quad E_2=\frac{m}{2}v_2^2,$$

where v_1 is the component of the positron velocity parallel to the axis of the flight tube, v_2 is the one normal to the axis, and m is the positron mass (Fig. 2). The angle of the positron velocity to the axis is

$$\theta\equiv\tan^{-1}\left(\frac{v_2}{v_1}\right)=\tan^{-1}\left(\frac{E_2}{E_1}\right)^{\frac{1}{2}}. \tag{2}$$

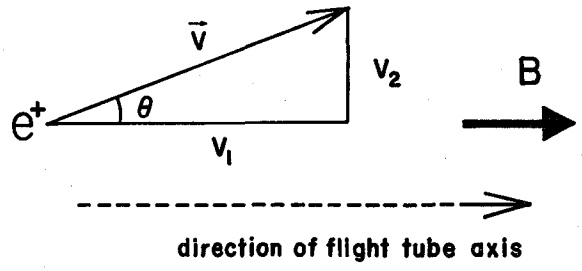

Fig. 2. Definitions of v_1 and v_2.

E_1 is measured by the conventional TOF methods,[2] and we will fix E_1 in the following discussion, so that we can regard E_2 as a variable which indicates the magnitude of the angle θ.

In order to obtain the E_2 distribution of the slow positrons, a homogeneous axial magnetic field B is applied. Then the slow positrons started from the slit at the left end of the flight tube travell to the right end of the tube, drawing helical paths with the radii

$$r_B(B, E_2)=\frac{(2mE_2)^{\frac{1}{2}}}{eB} \tag{3}$$

where e is the positron charge. For simplicity we assume that the slit is small enough that it can be regarded as a point on the axis of the tube, and assume that the times of flight are longer than a half period of the helical motion. Then the positrons which can reach to the end of the tube must have such radii of the helical motions that

$$r_B(B, E_2)<r_C, \tag{4}$$

where r_C means a half of the tube radius. From Eqs. (3) and (4) we obtain

$$E_2^m(B)=\frac{(eBr_C)}{2m}, \tag{5}$$

where $E_2'''(B)$ means the upper limit of the possible E_2 value of such positrons that can come to the end of the tube in the axial magnetic field B.

We can use relation (5) to determine the angular distribution, that is, the E_2 distribution of slow positrons, by varying B. Let $\Delta N[E_2', E_2'']$ be the number of slow positrons of which E_2 lie between E_2' and E_2'', then

$$\Delta N[E_2'''(B),\ E_2'''(B')] = N(B') - N(B) \quad (B' > B), \tag{6}$$

where N(B) and N(B') are the experimentally determined slow positron yields in the magnetic field B and B', respectively, fixing all the other experimental conditions.

Actually our positron detection system has an effective opening of 0.5 cm radius, which is smaller than the tube radius (1 cm), then the yields of the slow positrons *wave* as varying B, as shown in Fig. 3. This waving originates from an instrumetal basis and can be explained as follows. In the field B corresponding to the valley of the waving, the helical period τ_B and the flight time t_f correspoding to the given E_1 have the relation

$$t_f \cong \left(n + \frac{1}{2}\right)\tau_B \quad (n = 1,\ 2,\ 3,\ \cdots). \tag{7}$$

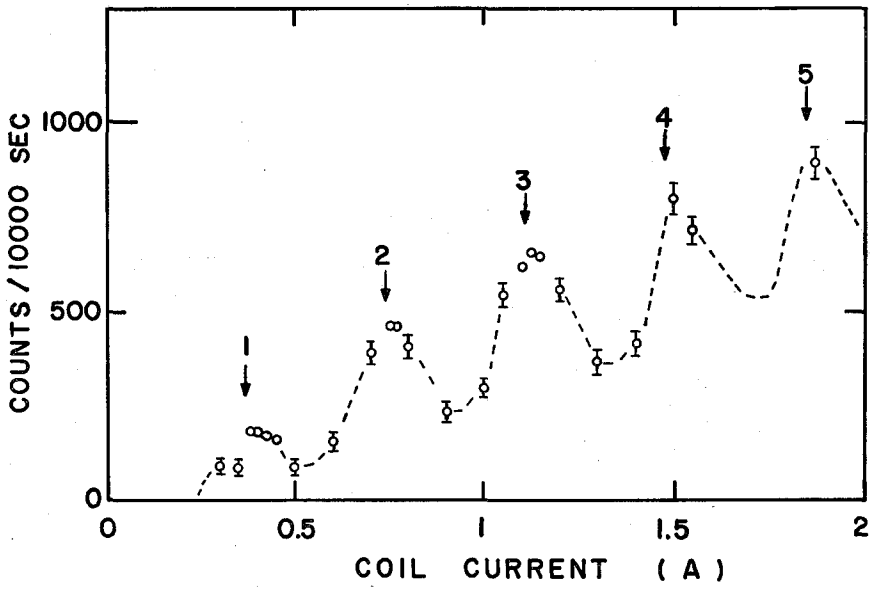

Fig. 3. Axial-magnetic-field dependence of the slow positron yields. Error bars indicate statistical errors only. For the circles without error bars the statistical errors are within the circles. Accumulation times: 10000 sec for 0.3, 0.35, 0.5, 0.6, 0.7, 0.8, 0.9, 1.0, 1.05, 1.2, 1.3, 1.4, 1.5, 1.55, and 1.88 A. 80000 sec for 0.38, 0.4, 0.42, 0.45, 0.75 0.77, 1.10, 1.13, and 1.15 A. The yields mean, the net counts of the slow positron peaks normalized to 10000 sec. Arrows and numbers indicate the positions where Eq. (8) or (10) is satisfied and the correspondent n values, respectively. The broken line is for eye guide.

Therefore, the slow positrons reach the tube end at the most distant position from the

tube axis, and some of them escape from the effective opening of the detection system. On the other hand in the field B corresponding to the peaks,

$$t_f \cong n\tau_B \quad (n=1, 2, 3, \cdots). \tag{8}$$

Therefore the positrons are focussed onto the center of the effective opening.

By the equations

$$t_f = \frac{l}{(2E_1/m)^{\frac{1}{2}}} \quad \text{and} \quad \tau_B = \frac{2\pi m}{eB}, \tag{9}$$

Equation (8) reduces to

$$B \cong \frac{2\pi n\,(2mE_1)^{\frac{1}{2}}}{el} \quad (n=1, 2, 3, \cdots), \tag{10}$$

where l is the flight path length. In the present analysis we can use as B or B′ in Eq. (6) only such B that satisfy Eq. (10), because in such cases the positrons which come to the end can be detected without loss. (Although the intrinsic efficiency of the detector has not been determined yet and may vary with the place of positron impact, but under the condition (8) or (10) the positrons will always hit an area of a few-mm diammeter near the center, and the effective efficiency, that is, the averaged value over such an area, could be treated as a certain constant. Consequently Eq. (6) doesn't lose the validity provided N and ΔN are regarded as relative values.)

RESULTS AND DISCUSSION

Typical TOF spectra are shown in Fig. 4. Slow positron peaks have been observed at $E_1 = 7.3 \pm 0.3$ eV with the full spreads ~ 2.2 eV.

In the present experiment the focussing condition (10) reduces to

$$I[\mathrm{A}] \cong 0.37n \quad (n=1, 2, 3, \cdots), \tag{11}$$

where I represents the coil current for the magnetic field ($B[\mathrm{T}] = 7.62 \times 10^{-4}\, I\,[\mathrm{A}]$) and the positions satisfying Eq. (11) are indicated by arrows in Fig. 3. Only the data near these arrows can be used to obtain E_2 distribution by Eq. (6), as discussed above. We adopt the data of which $I = 0.38$, 0.75, 1.10, 1.50, and 1.88 A.

Equation (5) reduces to

$$E_2^m(I) = (1.27^{+0.45}_{-0.37}) \times I^2 \tag{12}$$

in the present condition. The ambiguity essentially arises from the finite size of the right end slit.

Using Eqs. (6) and (12) with adopted data, we obtain the "E_2 spectrum" as follows,

$$\begin{aligned}
\Delta N(\ \ 0,\ 0.18) &= 186 \pm 9, \\
\Delta N(0.18,\ 0.71) &= 272 \pm 14, \\
\Delta N(0.71,\ 1.54) &= 161 \pm 16, \\
\Delta N(1.54,\ 2.86) &= 182 \pm 39, \\
\Delta N(2.86,\ 4.46) &= \ 93 \pm 52,
\end{aligned}$$

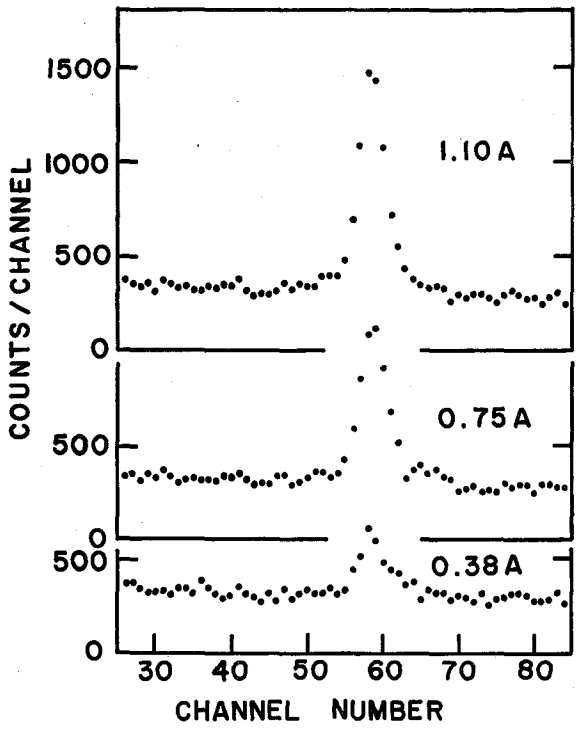

Fig. 4. Typical time-of-flight spectra.

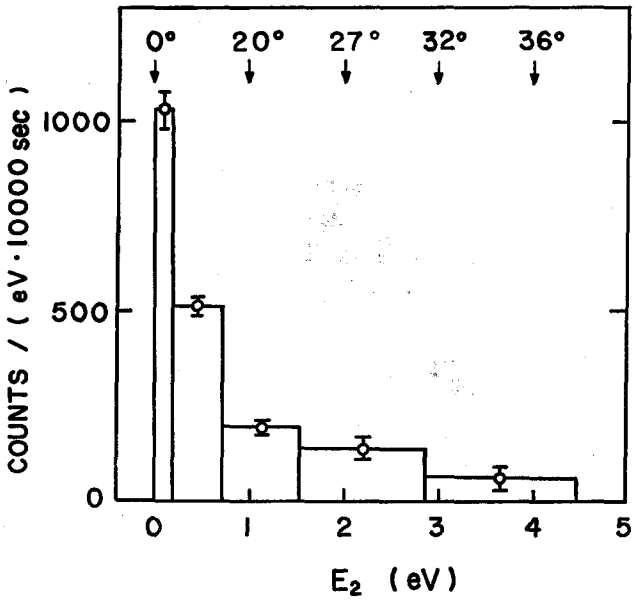

Fig. 5. E_2 spectrum. Error bars mean statistical errors only. Numbers with arrows indicate the angles to the axis $\theta \equiv \tan^{-1} (E_2/E_1)^{\frac{1}{2}}$, for $E_1 = 7.3$ eV. The area of each column represents the slow positron population.

where the units of the numbers in brackets and of the right hand sides are eV and positrons/10000 sec, respectively.

The attention must be paid, however, to the fact that true E_2 spectrum has been smeared over $\sim 1/3$ regions of each bin at the boundaries, due to the ambiguity of Eq. (12). These results are depicted as a histogram in Fig. 5.

E_2 spectrum of slow positrons from the present MgO moderator has shown an exponential-like curve, and representative E_2 value characterizing the curve would be ~ 1 eV (for example the average E_2 in the obtained five bins is 1.4 eV). From the results it is clear that, if the contribution of E_2 to E is not properly taken into account, there does exist a systematic error source of energy determination by TOF methods with the MgO moderator. In addition, the distribution of E_2 results in one of the limitation of the TOF energy resolution.

Thus we obtain an instruction that, to perform more precise and/or detailed experiments about slow positron collisions, the efforts of reducing E_2 are of essential importance.

ACKNOWLEDGMENTS

The authors are indebted to Emeritus Professor S. Shimizu for his encouragement. This work was partly supported by a Grant in Aid for Scientific Research of the Japanese Ministry of Education. This paper is dedicated to Professor Y. Takezaki in memory of his retirement.

REFERENCES

(1) T. C. Griffith and G. R. Heyland, *Phys. Rep.*, **39** (3), 169 (1978).
(2) Y. Nakayama, T. Mizogawa, and T. Kawaratani, *Bull. Inst. Chem. Res., Kyoto Univ.*, **58**, 88 (1980).